

## A NOVEL IMPEDANCE SOURCE INVERTER TOPOLOGY WITH ACTIVE FRONT-END FOR AC DRIVES

**D Bensiker Raja Singh**

Department of Electrical Engineering, Satyam College of Engineering, Kanyakumari, Tamil Nadu.  
Email: benzees003@gmail.com

**SujaManimalar R**

Department of Electrical Engineering, DMI College of Engineering, Chennai, Tamil Nadu.  
Email: sujamonimalar@gmail.com

**Abstract:** A unique impedance Source Inverter with an Active Front-End is proposed in this paper, that can be used for controlling AC Drives. There are a number of modulation schemes that may be used with the three-phase impedance source inverters, ultimate reduction in the switching losses makes the discontinuous modulation schemes seem most appropriate. The discontinuous modulation schemes are differentiated into two classes based on the technique used for achieving shoot-through (ST) state: single-phase-leg ST-based and three-phase-leg ST-based (3P) discontinuous modulation schemes. In this paper, we discuss the improvements in Single Phase Maximum Boost Discontinuous Space Vector modulation (1P/MB/DSVM) scheme under similar operating conditions, by simplifying gate signal generation and improving the conversion efficiency. A simulated analysis and comparison of the conventional and the enhanced 1P/MB/DSVM schemes is also discussed using PLECS. Lastly, verification of the simulation outcomes and reported analysis is carried out by making use of a three-phase quasi-Z-source inverter (qZSI) prototype which demonstrates improvement in conversion efficiency, utilizing the refined 1P/MB/DSVM scheme.

**Key words:** Impedance Source Inverter, Active-Front-End, Discontinuous Space Vector Modulation, Quasi-Z-Source inverter.

### I. INTRODUCTION

Interest in the renewable energy sources (RESs) has increased by many folds over the past few decades and they are now rapidly being incorporated into the power systems, stimulating an ongoing improvement in the power conditioning stage (PCS) with respect to the structures being used, their control schemes and modulation [1]–[4]. The boost converter-fed voltage source inverter (VSI) PCS, commonly known as the two-stage PCS, is essential in a few applications like fuel cells and photovoltaic (PV) devices, owing to the un-regulated output dc voltage [5]. A novel alternative to the common two-stage architecture is offered by the single-stage PCSs, demonstrated in the impedance source

Inverters [6]–[10]. The huge amount of attention being given to these impedance source inverters can be attributed to two elementary reasons. First, the

acceptance of the boosting capability in the inversion operation, meaning that they can function as buck-boost inverters and second, they can use an additional switching state, the shoot-through (ST) state that does not necessitate dead-time generation. The shoot-through (ST) state is allowed in these kinds of power inverters because of the use of an impedance network existing between the inverter three-phase-leg ST-based (3P) modulation schemes, which achieves the shoot-through state by utilizing the three phase-legs simultaneously; single-phase-leg ST-based (1P) modulation schemes, where the shoot-through state is achieved by using one phase-leg at a time. Moreover, these categories use both the continuous and dis-continuous modulation schemes, however, the discontinuous modulation scheme is deemed more valuable because of the resulting improvement in switching losses [14].

This paper deals with the single-phase-leg discontinuous modulation schemes with maximum boost (MB) capacity [14]– [16], with the proposal of a much improved 1P/MB discontinuous space vector modulation (1P/MB/DSVM). In comparison with the conventional 1P/MB/DSVM scheme, the modified version has the following advantages:

Smooth and easy generation of the gate signals, i.e. reduction in implementation difficulty; the switches alternating at the ST current for a shorter time period during the fundamental period; reduction in switching losses and enhancement in conversion efficiency.

The rest of this paper follows the scheme as given: Section II discusses the general operation of the three-phase qZSI and studies its modulation using the traditional 1P/MB/DSVM scheme. Section III introduces the advanced 1P/MB/DSVM scheme and presents a comparison with the conventional scheme. For verification of the previously reported analysis, Section IV addresses the results obtained by simulation, along with the calculated switching

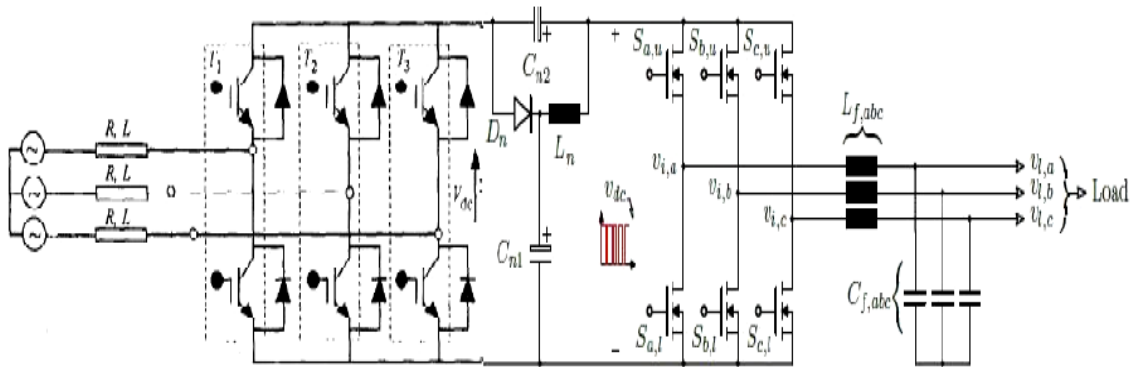


Fig. 1. Circuit diagram of the three-phase quasi-Z-source inverter (qZSI) with an output LC filter.

Losses, for the improved and the commonly used 1P/MB/DSVM schemes using PLECS. The experimental results obtained with a three-phase qZSI prototype are presented and discussed in Section V. The functionality of the modified 1P/MB/DSVM scheme is verified by these results and an improvement in conversion efficiency is demonstrated. Section VI deals with the conclusions drawn from the above results and discussion.

## II. REVIEW OF THE THREE-PHASE QZSI OPERATION AND MODULATION

### A. Operation of the Three-Phase qZSI

The three-phase qZSI shown in Fig. 1 uses an impedance network that consists of two inductors ( $2L_n$ ) of exactly the same kind, a diode ( $D_n$ ) and two capacitors ( $C_{n1}$  and  $C_{n2}$ ) between the input dc source ( $V_{in}$ ) and the B6-bridge used [8]. This impedance network makes it possible to use an additional switching state, known as the shoot-through (ST) state, during which the B6-bridge acts as a short circuit as shown in Fig. 2(a).

This B6-bridge, however, functions as a current source in the non-ST states as shown in Fig. 2(b).

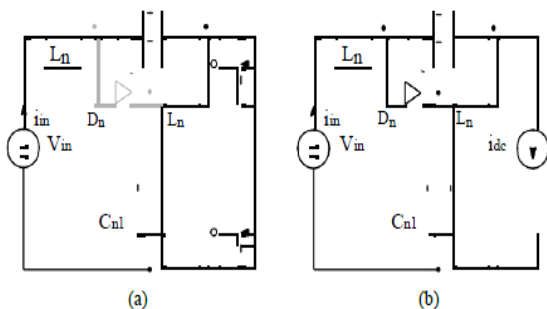


Fig. 2. Equivalent circuits of the qZSI during the ST and the non-ST states.

- (a) During the ST state and the B6-bridge becomes equivalent to a short circuit; and (b) during the non-ST states and the B6-bridge becomes equivalent to a current source.

A discontinuous dc-link voltage ( $v_{dc}$ ) results from such use of the ST state that pulsates between zero and a peak value of  $v^{dc}$  during a continuous conduction mode of operation. The peak value ( $v^{dc}$ ) is controlled by monitoring the ST state equivalent time. Another thing to be noted here is that this ST state has to be inserted within the zero states, i.e. the conventional zero states equivalent time is assigned partially or completely to the ST state so that it does not affect the active states and output voltage.

### B. Modulation of the Three-Phase qZSI

The qZSI shown in Fig. 1 is modulated under any modulation scheme, to get a three-phase symmetrical output voltage. The output fundamental peak phase voltage is given by:

$$\hat{V}_{\phi 1} = M \cdot \frac{\hat{v}_{dc}}{2}, \quad (1)$$

where  $M$  is the modulation index and  $v^{dc}$  is the peak dc-link voltage given by:

$$\hat{v}_{dc} = \frac{V_{in}}{1 - 2D_{ST}}, \quad (2)$$

$V_{in}$  being the input dc voltage and  $D_{ST}$  is the average of the ST duty cycle ( $d_{ST}$ ) that varies from one modulation scheme to another.

With the many different modulation schemes for modulation of qZSI have been mentioned, this paper

deals particularly with the conventionally used 1P/MB/DSVM scheme. The reference signals for said scheme are shown in Fig. 3. According to [14], [16], these reference signals are represented by:

$$\begin{aligned} v_{max,u}^* &= v_{max}^* \\ v_{max,l}^* &= v_{max}^* \\ v_{mid,u}^* &= v_{mid}^* \\ v_{mid,l}^* &= v_{mid}^* - d_{ST}, \\ v_{min,u}^* &= v_{min}^* - d_{ST}, \\ v_{min,l}^* &= v_{min}^* - 2d_{ST}, \end{aligned}$$

Where

$$\begin{aligned} v_{max}^* &= \max(v_a^*, v_b^*, v_c^*), \\ v_{mid}^* &= \text{mid}(v_a^*, v_b^*, v_c^*), \\ v_{min}^* &= \min(v_a^*, v_b^*, v_c^*), \\ v_{max,u}^* &= \max(v_{a,u}^*, v_{b,u}^*, v_{c,u}^*), \\ v_{max,l}^* &= \max(v_{a,l}^*, v_{b,l}^*, v_{c,l}^*), \\ v_{mid,u}^* &= \text{mid}(v_{a,u}^*, v_{b,u}^*, v_{c,u}^*), \\ v_{mid,l}^* &= \text{mid}(v_{a,l}^*, v_{b,l}^*, v_{c,l}^*), \\ v_{min,u}^* &= \min(v_{a,u}^*, v_{b,u}^*, v_{c,u}^*), \\ v_{min,l}^* &= \min(v_{a,l}^*, v_{b,l}^*, v_{c,l}^*), \end{aligned}$$

being  $v^*a$ ,  $v^*b$ , and  $v^*c$  are given by:

$$V^*a = 1;$$

$$v_b^* = 1 - M \cdot \left\{ \frac{3}{2} \sin(\omega_1 t) - \frac{\sqrt{3}}{2} \cos(\omega_1 t) \right\},$$

$$v_c^* = 1 - M \cdot \left\{ \frac{3}{2} \sin(\omega_1 t) + \frac{\sqrt{3}}{2} \cos(\omega_1 t) \right\},$$

Finally, the ST duty cycle ( $d_{ST}$ ) is variable during the fundamental period and it is given by:

$$d_{ST} = 1 - \frac{\sqrt{3}M}{2} \sin(\omega_1 t + \frac{\pi}{6}), \quad (4)$$

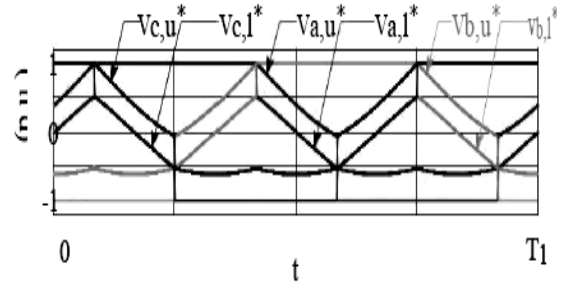


Fig. 3. Reference signals of the conventional single-phase-leg ST-based maximum boost discontinuous space vector modulation (1P/MB/DSVM) scheme, where the modulation index ( $M$ ) is equal to 0.7 and  $T_1$  is the fundamental period. Note that for any phase-leg  $x$ ,  $v_{x,u}$  is used to modulate  $S_{x,u}$ , while  $v_{x,l}$  is used to modulate  $S_{x,l}$ .

### III. MODIFIED DSVM SCHEME

It can be concluded from the prior discussions that the conventional 1P/MB/DSVM scheme, as shown in Fig 3, has the difficulty in generating the gate signals due to the complex calculation of the reference signals; despite the fact that the ST state is being inserted three times during the course of each switching cycle, effective switching frequency of the impedance network changes between one to three times the carrier frequency. This is because of the variation of the active states equivalent time. Thus, the impedance network must be designed based on the lowest value of the effective switching frequency. In addition, to the following disadvantages, for the upper switches, commutation at ST current takes place for around two-thirds of the fundamental period. In order to overcome these disadvantages, this paper proposes a modified and enhanced 1P/MB/DSVM scheme as given in Fig. 4. The modified 1P/MB/DSVM scheme uses

three reference signals that are commonly used with the traditional three-phase VSIs as shown in Fig. 4, and are given by (4). The three-phase qZSI can be modulated as follows using the improved 1P/MB/DSVM scheme: for any phase-leg  $x$ ,  $S_{x,u}$  is switched ON when  $v^*x$  is larger than the carrier signal, while  $S_{x,l}$  switches ON when  $v$  is smaller than the carrier signal or is the smallest reference signal as shown in Fig. 4. Hence, the ST is attained through phase-leg  $x$  when  $v_x$  is the smallest reference signal.

As a result of the improved 1P/MB/DSVM scheme, the lower switches never commutate at the

ST current, while the upper switches commute at ST-current for one-third of the fundamental period. The impedance network effective switching frequency is fixed at the carrier frequency. Whereas, the modified modulation scheme the same variable ST duty cycle (dST) as the conventional scheme. Where, dST and its average (DST) are given by (5). So,  $V_{in}$  is related to  $V_{\phi 1}$  using the previous equations (1) and (2) for the conventional scheme (1P/MB/DSVM). To design the impedance network properly based on the improved 1P/MB/DSVM scheme, the process followed in [8] can be used here also.

The estimated value of inductor and capacitor can be found by:

$$L_n \approx \frac{\sqrt{3M} \cdot V_{in}}{70\pi(3\sqrt{3M} - \pi) \cdot f_1 \cdot \Delta I_L} + \frac{3\sqrt{3M} \cdot (\pi - 3\sqrt{3M}) \cdot V_{in}}{4(3\pi\sqrt{3M} - \pi^2) \cdot f_s \cdot \Delta I_L},$$

$$C_{n1} \approx \frac{\sqrt{3M} \cdot I_{in}}{35\pi^2 \cdot f_1 \cdot \Delta V_{C_{n1}}} + \frac{(2\pi - 3\sqrt{3M}) \cdot I_{in}}{2\pi f_s \cdot \Delta V_{C_{n1}}},$$

$$C_{n2} \approx \frac{\sqrt{3M} \cdot I_{in}}{35\pi^2 \cdot f_1 \cdot \Delta V_{C_{n2}}} + \frac{(2\pi - 3\sqrt{3M}) \cdot I_{in}}{2\pi f_s \cdot \Delta V_{C_{n2}}},$$

where  $f_s$  is the switching frequency,  $I_{in}$  is the average input dc current,  $\Delta I_L$  is the peak-to-peak inductor current ripple, and  $\Delta V_{C_{n1}}$  and  $\Delta V_{C_{n2}}$  are the peak-to-peak capacitor voltage ripples across  $C_{n1}$  and  $C_{n2}$  respectively.

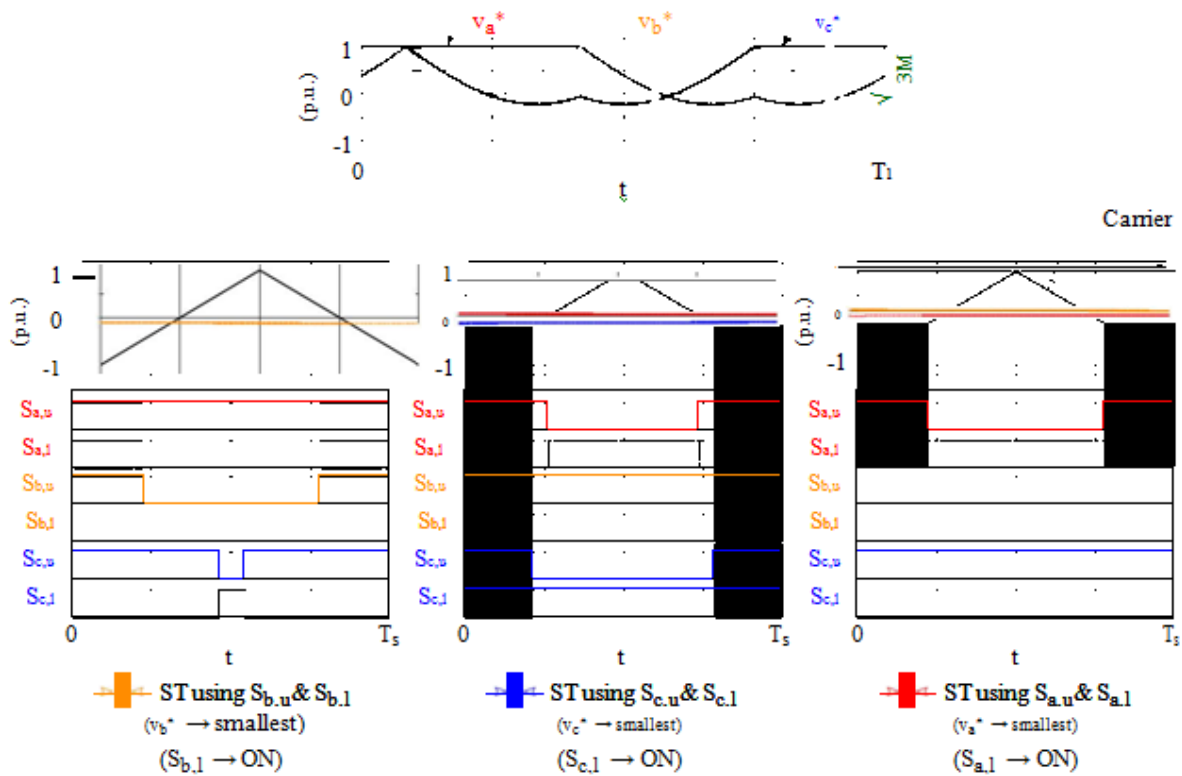


Fig. 4. Reference, carrier, and gate signals of the improved 1P/MB/DSVM scheme ( $M = 0.7$ ). Note that  $S_{a,l}$  is ma

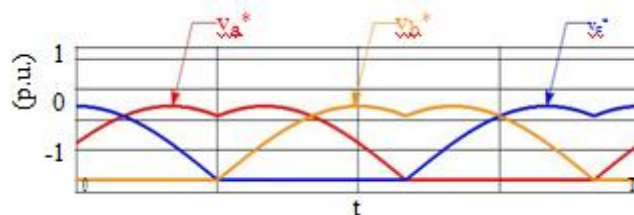


Fig. 5. Reference signals of the improved 1P/MB/DSVM scheme with negative dc clamping.

The fact that the improved 1P/MB/DSVM scheme is conceptually similar to the modulation scheme proposed in [11]. Whereas, the modified version proposed in [11], is not an discontinuous one.

The DSVM scheme may be attained with positive dc clamping that is used in this paper, or by negative dc clamping [14]. Taking into account the

reference signals of the modulated 1P/MB/DSVM scheme with negative dc clamping, this can be clarified. Fig. 5 shows this scheme in which the three-phase qZSI is modulated as follows: for a phase-leg x,  $S_{x;l}$  is turned ON when  $v_x$  is smaller than the carrier signal, while  $S_{x;u}$  is turned ON when  $V_x$  is larger than the carrier.

Table 1  
Comparison between the Conventional and the Improved DSVM schemes

	Conventional	Modified
Ref. signals	Fig. 3	Fig. 4
Num. of ref. signals	6	3
Complexity	High	Low
$S_{abc;l}$ unnormalized ST duration ( $T_{ST;l}/T_1$ )	$2/3$	$1/3$
$S_{abc;l}$ normalized ST duration ( $T_{ST;l}=T_1$ )	$1/3$	0

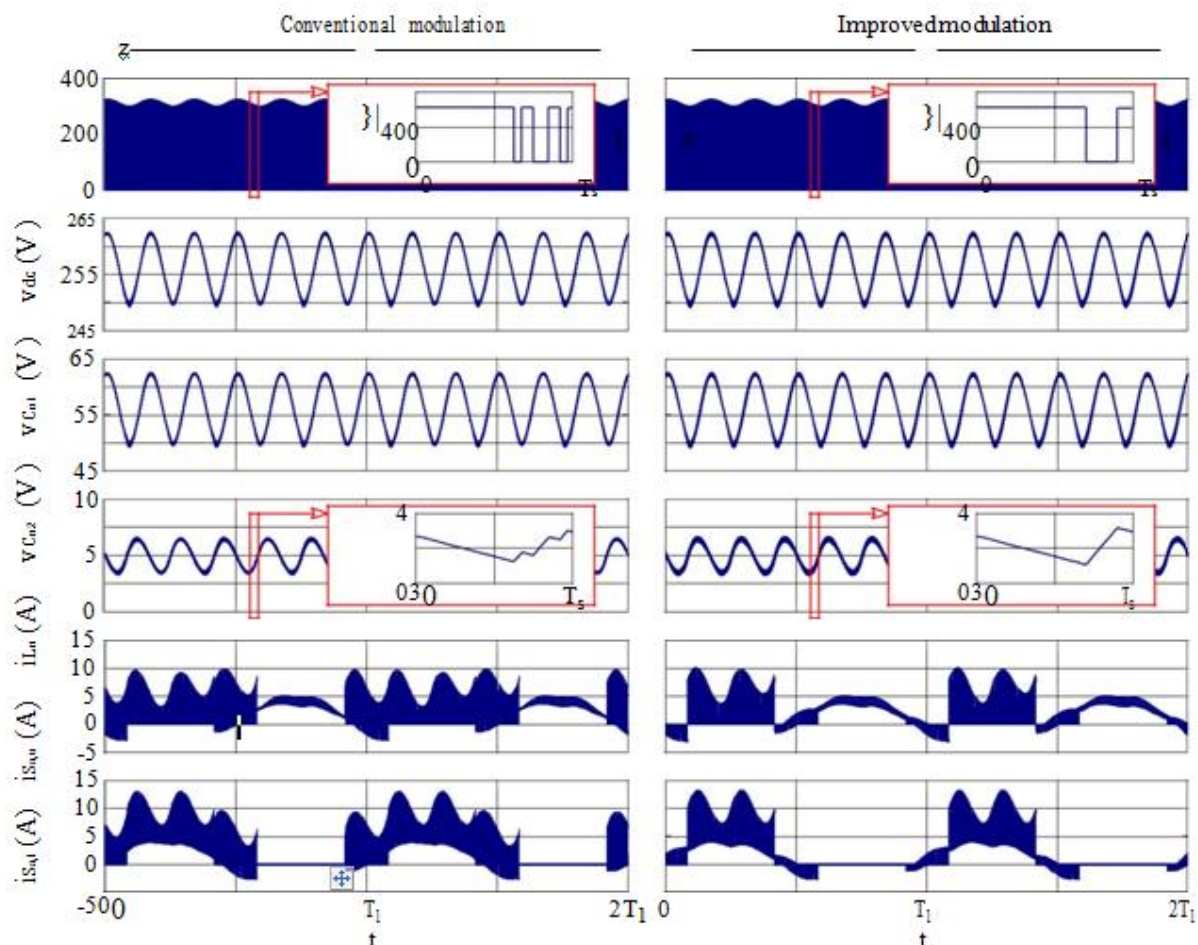


Fig. 6. Simulation results of the 1 kVA qZSI using the conventional and the improved 1P/MB/DSVM schemes. For each modulation scheme, the dc-link voltage ( $v_{dc}$ ), impedance network capacitors voltages ( $v_{Cn1}$  and  $v_{Cn2}$ ), impedance network inductor current ( $i_{Ln}$ ), and upper and lower switches currents of phase a ( $i_{Sa;u}$  and  $i_{Sa;l}$ ) are shown from top to bottom.



Table 2  
Simulation Parameters (1000 VA Three-Phase QZSI)

$V_{in}$	200 V	$V'_1$	110 V (RMS)	M	0:8564
$f_s$	60 kHz	$L_n$	1:6 mH	Cn1;2	20 F
$f_1$	200 Hz	Lf;abc	0:35 mH	Cf;abc	4:7 F

$v_x$  is greater than the carrier signal, or is the largest reference signal,.

A. Comparative Study

Table I presents a comparison of both schemes from various different aspects, including number of reference signals, , normalized peak dc-link voltage ( $v^{dc}=V_{in}$ ), ST duty cycle (dST ) variation, average ST duty cycle (DST ), implemen-tation complexity,

normalized ST duration for the upper switches (TST;u=T1) normalized output fundamental peak phase voltage ( $V'_1=V_{in}$ ) and and normalized ST duration for the lower switches (TST;l=T1). It highlights and summarizes the complete difference between the conventional and improved scheme.

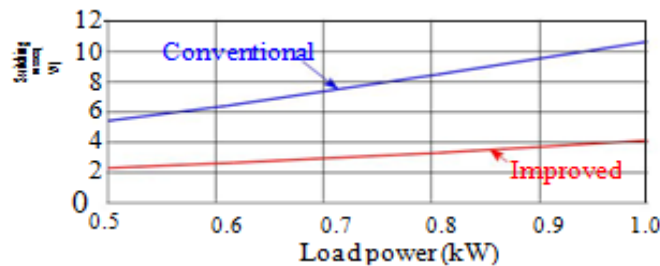


Fig. 7. Simulated total switching losses of the B6-bridge using PLECS for both the conventional and the improved 1P/MB/DSVM schemes. Note that the utilized switch model is C2M0025120D from CREE.

Table Imakes it evident that the improved 1P/MB/DSVM scheme does in-fact enhance the performance of the three-phase qZSI, which is attributed to the smaller ST duration of the various switches, reducing the overall switching losses for the same point of operation.

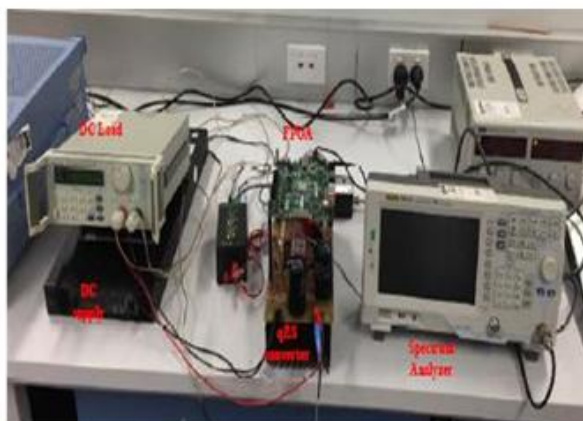


Fig. 8. Experimental prototype of the three-phase ZSI with an output LC filter.

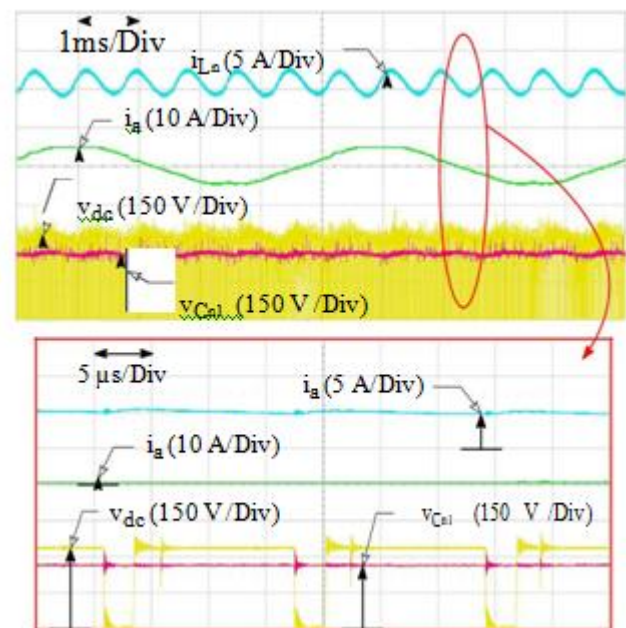


Fig. 9. Obtained experimental results using the proposed modulation scheme using a resistive load of 1 kW, where the dc-link voltage ( $v_{in}$ ), voltage across Cn1 ( $v_{Cn1}$  ), inductor current ( $i_{Ln}$  ), and load current ( $i_a$ ) are shown with a zoom for three switching cycles.

#### IV. SIMULATION RESULTS

For verification of the previous analysis and discussions, a 1 kVA qZSI, the parameters of which are enlisted in Table II, was simulated using PLECS. A resistive load (RL) was fed by this qZSI via an LC filter as depicted in Fig. 1. The value of M was set to 0:8564 to get a fundamental RMS output phase voltage ( $V_1$ ) equivalent to 110 V .

Fig. 6 depicts the simulation based data results using both the conventional and the improved 1P-ST/MB/DSVM schemes,

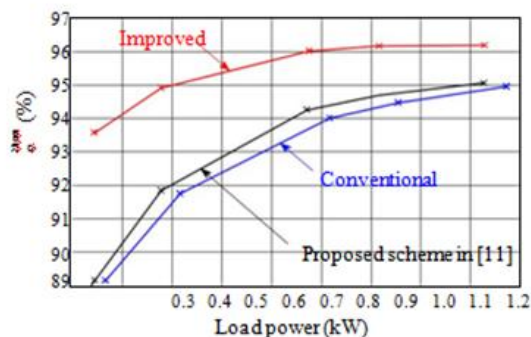


Fig. 10. Measured experimental efficiency of the three-phase qZSI for the conventional and the improved 1P/MB/DSVM schemes, and the introduced modulation scheme in [11].

where the impedance network inductor current, dc-link voltage ( $v_{dc}$ ), impedance network capacitors voltages ( $v_{Cn1}$  and  $v_{Cn2}$ ),

( $i_{Ln}$ ), as well as upper and lower switch currents of phase a ( $i_{Sa;u}$  and  $i_{Sa;l}$ ) are shown for both schemes.

The prior analysis is confirmed by these results and the effective functionality of the proposed modulation scheme is supported. Studying the difference in results for both kinds of schemes (Fig. 6) shows that the modified 1P/MB/DSVM scheme works the same way as the conventional 1P/MB/DSVM scheme with an overall improvement in performance.

This performance improvement can be attributed to the simplicity of the different switches and the reduction in commutation periods at the ST current, which is evident from the represented switch currents ( $i_{Sa;u}$  and  $i_{Sa;l}$ ) in Fig. 6. Additionally, it is evident from the inductor current ( $i_{Ln}$ ) and dc-link voltage ( $v_{inv}$ ) using both schemes, that

effective switching frequency for the 1P/MB/DSVM scheme commonly in practice varies between one to three times the frequency of the carrier, while for the modified 1P/MB/DSVM scheme it remains constant and it is equivalent to the carrier frequency.

Finally, the switching losses have been calculated using PLECS for both modulation schemes at different load conditions, where the obtained results are shown in Fig. 7. This figure, i.e. Fig. 7, shows that the switching losses under the improved scheme has been significantly reduced due to the shorter periods of commutation at the ST current.

#### V. EXPERIMENTAL RESULTS

Verification of the improved 1P/MB/DSVM scheme functionality was carried out using a three-phase ZSI prototype, shown in Fig. 8. The prototype parameters are as listed in Table II.

The prototype was tested at 1 kW using the modified 1P/MB/DSVM scheme and the recorded results are shown in Fig. 9, in which the inductor current ( $i_{Ln}$ ), dc-link voltage ( $v_{dc}$ ), voltage across  $C_{n1}$  ( $v_{Cn1}$ ), and load current ( $i_a$ ) are shown along with a zoom for three switching cycles. These results validate the functionality of the modified 1P/MB/DSVM scheme and verify the given simulation results.

The conversion efficiency of the three-phase ZSI prototype was measured under both the conventional and modified 1P/MB/DSVM schemes, using a KinetiQ PPA5530 power analyser and the measurements obtained are shown in Fig. 10. This figure confirms the advantage of enhancing the converter efficiency due to the shorter commutation period at the ST current. Moreover, the conversion efficiency under the introduced improved modulation scheme in [11] was measured and showed in Fig. 10, which shows that the improved 1P/MB/DSVM scheme exhibits higher efficiency owing to the smaller voltage stresses of the MB as well as the discontinuity of the modulating the switches. This prototype was based on a CCS050M12CM2 SiC power module and a C4D40120D SiC diode from CREE.

#### VI. CONCLUSION

This paper introduces a unique Z-Source with active front-End, that is validated by simulation and experimental setup.

The conventional (1P/MB/DSVM) scheme has been studied and improved upon to increase the conversion efficiency and enhance the performance of the three-phase impedance source inverters. The improved 1P/MB/DSVM scheme has the following benefits over the conventional scheme: easier to implement because it uses three reference signals, the switches commute for shorter period at the ST current during the fundamental period, thereby achieving reduced switching losses and consequently better efficiency.

The modified 1P/MB/DSVM scheme has been introduced and analyzed in compared to the conventional scheme. The switching losses were recalculated using PLECS for both kinds of schemes, with the modified scheme exhibiting an effective reduction in switching losses. Finally, experimental results verify the reported analysis by making use of a three-phase quasi-Z-source inverter (qZSI) prototype, and the results showed an increase in the conversion efficiency with the usage of the improved 1P/MB/DSVM scheme under the same operating conditions.

#### References

- [1] F. Blaabjerg, K. Ma, and Y. Yang, "Power electronics - the key Technology for renewable energy systems," in Ninth Int. Conf. on Ecological Vehicles and Renewable Energies (EVER), Mar. 2014, pp. 1–11.
- [2] F. Blaabjerg, Y. Yang, D. Yang, and X. Wang, "Distributed power generation systems and protection," Proc. of the IEEE, vol. 105, no. 7, pp. 1311–1331, July 2017.
- [3] Abdelhakim, P. Mattavelli, D. Yang, and F. Blaabjerg, "Coupled inductor-based dc current measurement technique for transformerless grid-tied inverters," IEEE Trans. on Power Electron., vol. 33, no. 1, pp. 18–23, Jan 2018.
- [4] Abdelhakim, P. Mattavelli, V. Boscaino, and G. Lullo, "Decoupled control scheme of grid-connected split-source inverters," IEEE Trans. on Ind. Electron., vol. 64, no. 8, pp. 6202–6211, Aug 2017.
- [5] J. M. Carrasco, L. G. Franquelo, J. T. Bialasiewicz, E. Galvan, R. C. PortilloGuisado, M. A. M. Prats, J. I. Leon, and N. Moreno-Alfonso, "Power-electronic systems for the grid integration of renewable energy sources: A survey," IEEE Trans. on Ind. Electron., vol. 53, no. 4, pp. 1002–1016, June 2006.
- [6] Abdelhakim, P. Mattavelli, and G. Spiazzi, "Three-phase split source inverter (ssi): Analysis and modulation," IEEE Trans. on Power Electron., vol. 31, no. 11, pp. 7451–7461, Nov. 2016.
- [7] Abdelhakim, P. Davari, F. Blaabjerg, and P. Mattavelli, "Switching loss reduction in the three-phase quasi-z-source inverters utilizing modified space vector modulation strategies," IEEE Trans. on Power Electron., vol. PP, no. 99, pp. 1–1, 2017.
- [8] M. Shen, A. Joseph, J. Wang, F. Z. Peng, and D. J. Adams, "Comparison of traditional inverters and z-source inverter for fuel cell vehicles," IEEE Trans. on Power Electron., vol. 22, no. 4, pp. 1453–1463, July 2007.
- [9] Abdelhakim, P. Mattavelli, P. Davari, and F. Blaabjerg, "Performance evaluation of the single-phase split-source inverter using an alternative dc-ac configuration," IEEE Trans. on Ind. Electron., vol. PP, no. 99, pp. 1–1, 2017.
- [10] Abdelhakim, P. Davari, F. Blaabjerg, and P. Mattavelli, "An improved modulation strategy for the three-phase z-source inverters (zsis)," in IEEE Energy Conv. Cong. and Expo. (ECCE), Oct 2017, pp. 4237–4243.
- [11] M. Zdanowski, D. Peftitsis, S. Piasecki, and J. Rabkowski, "On the design process of a 6-kva quasi-z-inverter employing sic power devices," IEEE Trans. on Power Electron., vol. 31, no. 11, pp. 7499–7508, Nov 2016.
- [12] Y. P. Siwakoti, F. Z. Peng, F. Blaabjerg, P. C. Loh, G. E. Town, and S. Yang, "Impedance-source networks for electric power conversion part II: Review of control and modulation techniques," IEEE Trans. on Power Electron., vol. 30, no. 4, pp. 1887–1906, April 2015.
- [13] P. C. Loh, D. M. Vilathgamuwa, Y. S. Lai, G. T. Chua, and Y. Li, "Pulse-width modulation of z-source inverters," IEEE Trans. on Power Electron., vol. 20, no. 6, pp. 1346–1355, Nov. 2005.
- [14] F. Z. Peng, M. Shen, and Z. Qian, "Maximum boost control of the z-source inverter," IEEE Trans. on Power Electron., vol. 20, no. 4, pp. 833–838, July 2005.
- [15] Y. Zhang, J. Liu, X. Li, X. Ma, S. Zhou, H. Wang, and Y. Liu, "An improved pwm strategy for z-source inverter with maximum boost capability and minimum switching frequency," IEEE Trans. on Power Electron., vol. PP, no. 99, pp. 1–1, 2017.